NASA/TM—2004-212920

Successful Surface Treatments for Reducing Instabilities in Advanced Nickel-Base Superalloys for Turbine Blades

Ivan E. Locci
Case Western Reserve University, Cleveland, Ohio

Rebecca A. MacKay
Glenn Research Center, Cleveland, Ohio

Anita Garg
University of Toledo, Toledo, Ohio

Frank Ritzert
Glenn Research Center, Cleveland, Ohio

March 2004

The NASA STI Program Office . . . in Profile

Since its founding, NASA has been dedicated to the advancement of aeronautics and space science. The NASA Scientific and Technical Information (STI) Program Office plays a key part in helping NASA maintain this important role.

The NASA STI Program Office is operated by Langley Research Center, the Lead Center for NASA's scientific and technical information. The NASA STI Program Office provides access to the NASA STI Database, the largest collection of aeronautical and space science STI in the world. The Program Office is also NASA's institutional mechanism for disseminating the results of its research and development activities. These results are published by NASA in the NASA STI Report Series, which includes the following report types:

- TECHNICAL PUBLICATION. Reports of completed research or a major significant phase of research that present the results of NASA programs and include extensive data or theoretical analysis. Includes compilations of significant scientific and technical data and information deemed to be of continuing reference value. NASA's counterpart of peer-reviewed formal professional papers but has less stringent limitations on manuscript length and extent of graphic presentations.

- TECHNICAL MEMORANDUM. Scientific and technical findings that are preliminary or of specialized interest, e.g., quick release reports, working papers, and bibliographies that contain minimal annotation. Does not contain extensive analysis.

- CONTRACTOR REPORT. Scientific and technical findings by NASA-sponsored contractors and grantees.

- CONFERENCE PUBLICATION. Collected papers from scientific and technical conferences, symposia, seminars, or other meetings sponsored or cosponsored by NASA.

- SPECIAL PUBLICATION. Scientific, technical, or historical information from NASA programs, projects, and missions, often concerned with subjects having substantial public interest.

- TECHNICAL TRANSLATION. English-language translations of foreign scientific and technical material pertinent to NASA's mission.

Specialized services that complement the STI Program Office's diverse offerings include creating custom thesauri, building customized databases, organizing and publishing research results . . . even providing videos.

For more information about the NASA STI Program Office, see the following:

- Access the NASA STI Program Home Page at ***http://www.sti.nasa.gov***

- E-mail your question via the Internet to help@sti.nasa.gov

- Fax your question to the NASA Access Help Desk at 301–621–0134

- Telephone the NASA Access Help Desk at 301–621–0390

- Write to:
  NASA Access Help Desk
  NASA Center for AeroSpace Information
  7121 Standard Drive
  Hanover, MD 21076

NASA/TM—2004-212920

Successful Surface Treatments for Reducing Instabilities in Advanced Nickel-Base Superalloys for Turbine Blades

Ivan E. Locci
Case Western Reserve University, Cleveland, Ohio

Rebecca A. MacKay
Glenn Research Center, Cleveland, Ohio

Anita Garg
University of Toledo, Toledo, Ohio

Frank Ritzert
Glenn Research Center, Cleveland, Ohio

National Aeronautics and
Space Administration

Glenn Research Center

March 2004

Acknowledgments

Dr. R.A. MacKay would like to acknowledge many useful discussions with Dr. R. Grylles, formerly of General Electric Aircraft Engines. Excellent technical support from Robert Angus, Raymond Babuder, Anna Palczer, William Karpinski, Gary Kostyak, Myles McQuater, and Joy Buehler is also acknowledged and greatly appreciated. Special thanks to Dr. J.A. Nesbitt for reviewing this manuscript. This project was funded by the Ultra-Efficient Engine Technology program under Task 4.2.2.

Available from

NASA Center for Aerospace Information
7121 Standard Drive
Hanover, MD 21076

National Technical Information Service
5285 Port Royal Road
Springfield, VA 22100

Available electronically at http://gltrs.grc.nasa.gov

Successful Surface Treatments for Reducing Instabilities in Advanced Nickel-Base Superalloys for Turbine Blades

Ivan E. Locci
Case Western Reserve University
Cleveland, Ohio 44106

Rebecca A. MacKay
National Aeronautics and Space Administration
Glenn Research Center
Cleveland, Ohio 44135

Anita Garg
University of Toledo
Toledo, Ohio 43606

Frank J. Ritzert
National Aeronautics and Space Administration
Glenn Research Center
Cleveland, Ohio 44135

Summary

An optimized carburization treatment has been developed to mitigate instabilities that form in the microstructures of advanced turbine airfoil materials. Current turbine airfoils consist of a single crystal superalloy base that provides the mechanical performance of the airfoil, a thermal barrier coating (TBC) that reduces the temperature of the base superalloy, and a bondcoat between the superalloy and the TBC, that improves the oxidation and corrosion resistance of the base superalloy and the spallation resistance of the TBC. Advanced nickel-base superalloys containing high levels of refractory metals have been observed to develop an instability called secondary reaction zone (SRZ), which can form beneath diffusion aluminide bondcoats. This instability between the superalloy and the bondcoat has the potential of reducing the mechanical properties of thin-wall turbine airfoils. Controlled gas carburization treatments combined with a prior stress relief heat treatment and adequate surface preparation have been utilized effectively to minimize the formation of SRZ. These additional processing steps are employed before the aluminide bondcoat is deposited and are believed to change the local chemistry and local stresses of the surface of the superalloy. This paper presents the detailed processing steps used to reduce SRZ between platinum aluminide bondcoats and advanced single crystal superalloys.

Introduction

Current turbine airfoils consist of a single crystal superalloy base that provides the mechanical performance of the airfoil, a thermal barrier coating (TBC) that reduces the temperature of the base superalloy, and a bondcoat between the superalloy and the TBC that improves the oxidation and corrosion resistance of the base superalloy and improves the spallation resistance of the TBC. Advanced single-crystal superalloys containing high levels of refractory metals are susceptible to the formation of secondary reaction zone (SRZ), which can develop beneath diffusion aluminide coatings (refs. 1 to 4). SRZ is a microstructural instability that occurs during high temperature exposure and may form as a continuous layer or in discrete regions beneath the coating. SRZ has also been observed (refs. 1 and 2)

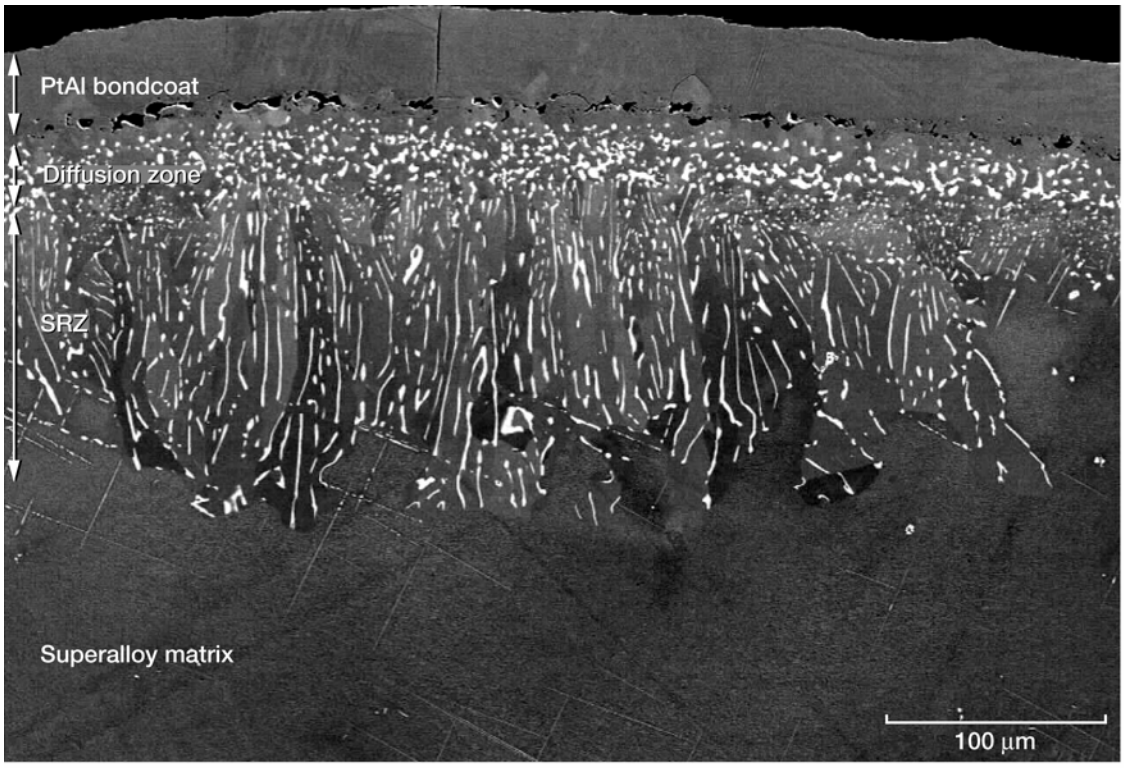

Figure 1.—Field emission scanning electron microscope (FESEM) image showing a secondary reaction zone (SRZ) formation beneath the diffusion zone of a PtAl-coated, refractory-rich superalloy after a long-term age at 1093 °C for 400 hr.

internally in some superalloys, but that form of SRZ will not be discussed in the present paper. Figure 1 shows a platinum aluminide (PtAl) bondcoat and the diffusion zone that normally develops between the bondcoat and the superalloy substrate. Beneath the diffusion zone lies the SRZ, which in this case may be seen as a nearly continuous layer. Figure 2 shows that SRZ is comprised of topologically close-packed (TCP) phases and stringers of γ in a matrix of γ'. The TCP and γ stringers tend to be aligned perpendicular to the growth interface, which is seen in figure 2 separating the SRZ from the single crystal superalloy.

The rhenium (Re) content of the superalloy, the inward diffusion of aluminum from the coating, and the surface stresses of the superalloy have been cited (refs. 1 and 2) as the key factors influencing the propensity of the alloy to form SRZ. Numerous surface modifications (ref. 1) have been studied in an attempt to reduce SRZ in alloys containing high Re contents. The use of gas carburization was envisioned and patented by GE Aircraft Engines (ref. 5) as a means to reduce SRZ under bondcoats. The deposition and diffusion of carbon into the superalloy surfaces was shown to cause submicron tantalum (Ta)-rich carbides to form, which changed the surface chemistry prior to bondcoat application. The carburization technique was subsequently employed to reduce SRZ during the development of single crystal alloys in the Enabling Propulsion Materials (EPM) program (ref. 3), but the effectiveness of the carburization varied greatly when the technique was performed in large scale facilities at commercial vendors. A carburization facility was established on a laboratory scale at Glenn Research Center after the end of the EPM program, so that key processing variables could be studied in more detail.

The present paper describes the details of the processing methods used and optimized at NASA Glenn Research Center for mitigating SRZ in advanced superalloy compositions that are highly susceptible to the formation of SRZ. Numerous surface finishes were prepared and examined to determine which contributed to the most effective carburization in several different types of specimens. The present study has also used a stress relief heat treatment prior to the carburization process; the former is believed to

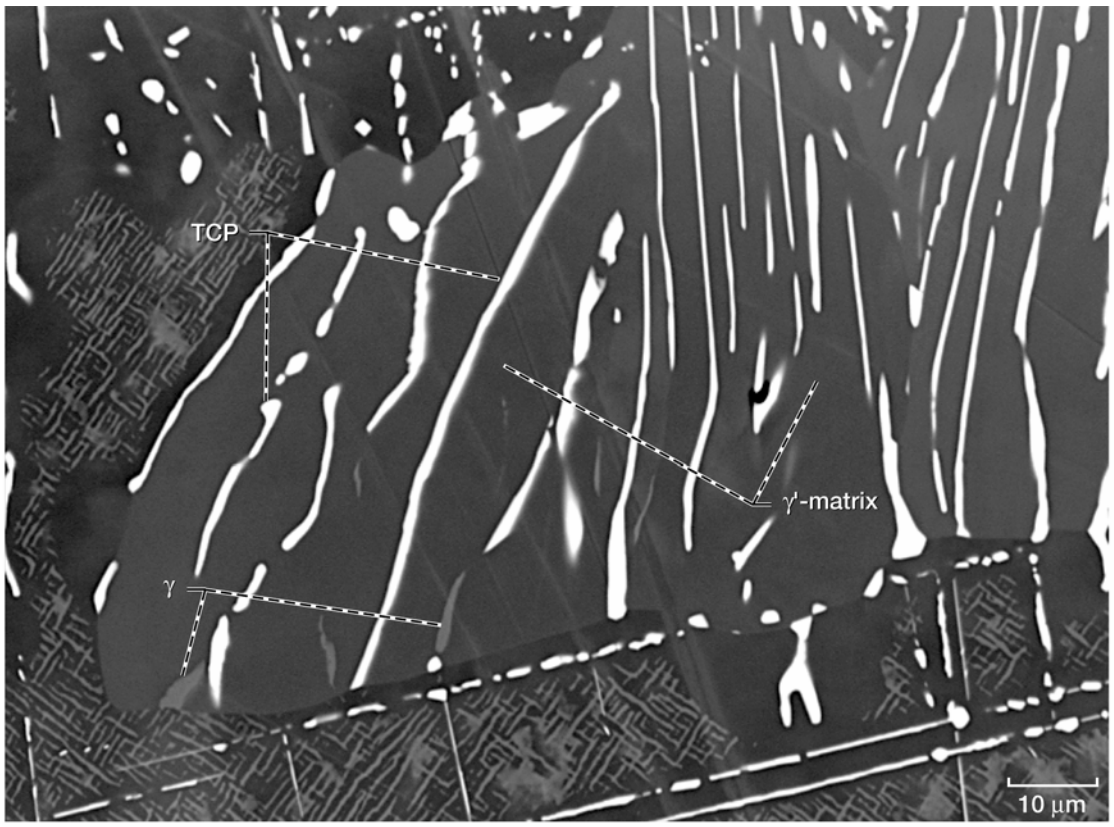

Figure 2.—FESEM image showing a higher magnification of secondary reaction zone (SRZ) formation. The SRZ is a three-phase constituent consisting of a γ' matrix with TCP and stringers of γ.

reduce surface stresses (refs. 3 and 4) by recrystallizing a thin layer on the superalloy surface. Results will be shown for single crystal slabs, machined test specimens, and full-scale commercial turbine blades.

Materials and Experimental Procedures

Material

Surface treatments in this study were conducted on single crystal slab material, mechanical test specimens machined from slab, and CF6-80E high pressure turbine (HPT) blades. The slabs and blades were cast from the advanced fourth-generation single-crystal superalloy EPM 102, which was developed in the High Speed Research – Enabling Propulsion Materials Program (ref. 3). Single crystal slabs (15.2 high by 5.1 wide by 1.5 cm thick) were cast and solution treated at 1315 °C for 6 hr at a commercial vendor, PCC-Minerva. The slabs were then grit blasted, chemically etched, and electrolytically etched to reveal low angle grain boundaries and other grain defects. The HPT blades underwent similar processing. Sections (1 high by 1 wide by 1.5 cm thick) were cut from slabs using a high speed wafering saw with a silicon carbide (SiC) blade, and test specimens were machined by slow-speed grinding from slabs before surface treatments were conducted. In addition, full-size blades and 1-cm high sections cut from blades were also used in this study. Examples of these specimen configurations are shown in figure 3.

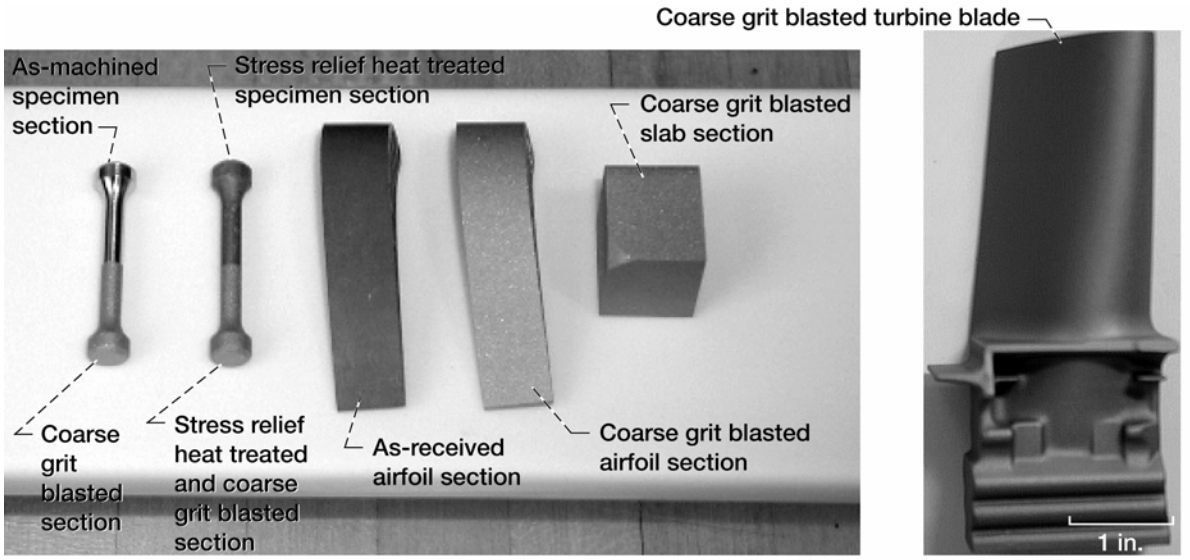

Figure 3.—Machined test specimens, airfoil sections, slab section, and full size turbine blade were prepared with various surface finishes prior to carburization. Note that each half of the machined test specimens has a different surface treatment.

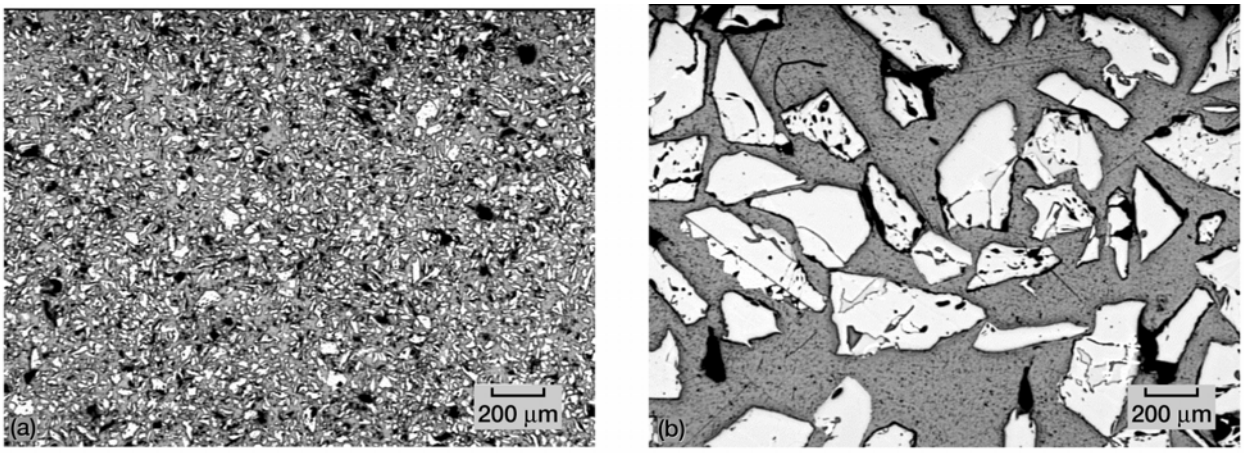

Figure 4.—Typical aluminum oxide media used for grit blasting the surface of the superalloy before carburization. (a) Fine grade (~50 μm, average size). (b) Coarse grade (~200 μm, average size).

Surface Finish Study

To determine an appropriate surface condition for effective carburization, slab sections with different surface finishes were prepared. Metallographic polishing on 1, 15, and 250 μm media was conducted. Other samples were manually grit blasted with either 50 or 200 μm (average size) alumina (Al_2O_3) particles at a 40 psi inlet air pressure and a nozzle diameter of 1.3 cm. Grit blasting was performed such that each specimen surface was covered a minimum of three times, with each pass lasting approximately 2 min. The grit blasting that used 50 μm Al_2O_3 media will be termed, "fine blasting," and the grit blasting that used 200 μm Al_2O_3 media will be termed, "coarse blasting," in the remainder of this report. Typical grit blasting media metallographically mounted and observed in an optical light microscope, is shown in figure 4. For comparison, other samples were left in the as-received surface condition or in the as-cut condition. After the desired surface preparations were obtained, the samples were ultrasonically cleaned

in acetone, and then in ethanol, and were air-dried and weighed. Samples were handled with gloves to prevent contamination prior to carburization.

Surface roughness was measured on selected samples using a Dektac[3] ST surface profile measuring system. The arithmetic average roughness, Ra, was used in this study to compare surface finishes produced prior to carburization. Ra is universally accepted as the international parameter of roughness (ref. 6); it is defined as the average deviation of the profile from the mean line and does not differentiate peaks from valleys. Ten random profile passes were made to obtain an average roughness value for each slab sample. Surface roughness measurements of the tensile and blade samples were more difficult to obtain due to the surface curvature present in each type of specimen; two to three passes were made with the profilometer to obtain an Ra for each of these specimens. The optimum surface preparation technique was subsequently chosen based on the uniformity and depth of carbide precipitation.

Carburization Cycle

Carburization was conducted in an Al_2O_3 tube furnace that could safely handle pure hydrogen (H_2) or H_2-rich gas mixtures. Samples were placed in a platinum basket to expose as much of the specimen surface area as possible to the flowing atmosphere. The basket, in turn, was placed on a high-purity Al_2O_3 boat which was then moved to the middle of the furnace hot zone. The furnace was purged with argon at 21 MPa, and then pumped down to at least 66 Pa and backfilled with argon. This sequence was repeated two more times to remove oxygen from the system.

The initial heat up of the samples to be carburized was conducted in pure H_2 so that the surfaces of the samples would be free of oxides or other contaminants that could interfere with the carburization at the surface. However, extra precautions had to be undertaken in order to operate under this environment due to the explosive nature of H_2 when it is mixed with oxygen. The system was leak checked with helium at 28 MPa and then purged with helium overnight before the system was purged with H_2 for one hour at ambient temperature prior to the start of the carburization cycle.

Figure 5 is a schematic illustrating the typical heating cycle used for carburization. The introduction of various gas mixtures is also indicated in the figure. The samples in the tube furnace were heated under H_2 from ambient temperature to 1060 °C. After a 10 min soak at 1060 °C, a gas mixture (in volume) of 3.5% H_2, 0.35% methane (CH_4), and 96.15% argon (Ar) was introduced to begin the carburization stage.

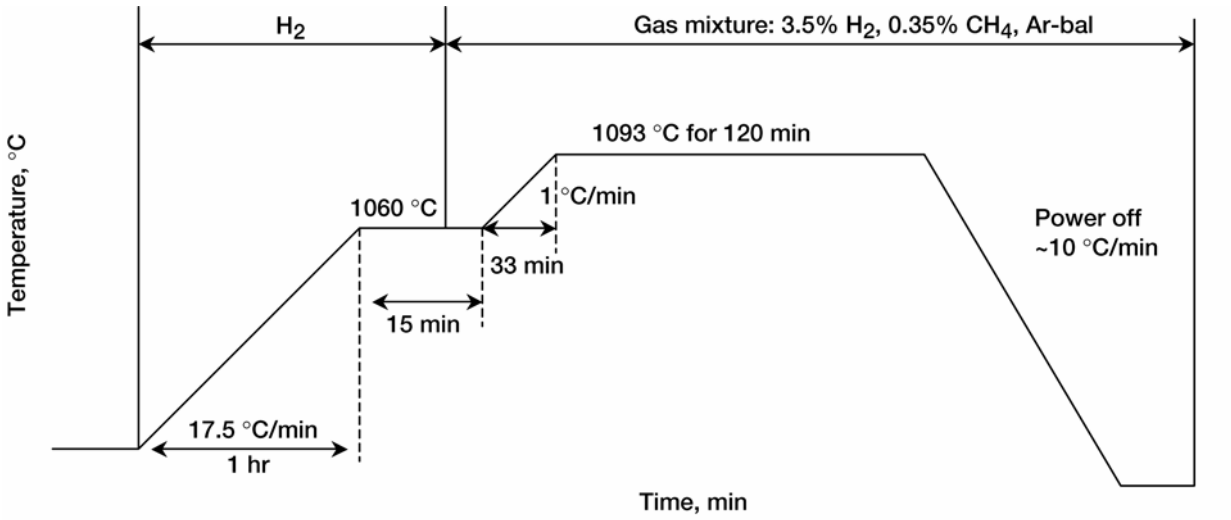

Figure 5.—Typical carburization cycle used. Temperature and time axes are not drawn to scale. Introduction of gases is superimposed wherever appropriate.

This mixture flowed continuously through the tube for the remainder of the heating and cooling cycles. The furnace was held for an additional 5 min to stabilize the temperature at 1060 °C, as the gas mixture was introduced, before ramping to 1093 °C in approximately 33 min. The typical final soak was for 2 hr at 1093 °C. Then the samples were slowly furnace-cooled to room temperature. At ambient temperature, helium was re-introduced and allowed to flow for 30 min so that the system could be opened safely to the atmosphere. Samples were removed with gloves and weighed. The weighing of the samples provided a first indication of a successful carburization. Normalized weight gains of the slabs were obtained by dividing the weight gain by the specimen surface area. The furnace was subsequently baked out in air at 1300 °C for 5 hr in order to burn any residual carbon in the Al_2O_3 tube prior to the next run.

Different temperatures and durations of the final soak in the carburization cycle were also investigated in an attempt to optimize the carburization depth. Other portions of the cycle remained unchanged. Specifically, final soaks at 982, 1066, or 1093 °C were examined with durations of either 2 or 4 hr.

After carburization was completed, samples were prepared metallographically in cross-sections extending from the surface through the depth of the sample. Samples were examined subsequently by high resolution field emission scanning electron microscopy (Hitachi FESEM), in its lower secondary electron detector mode. The targeted carbide depth was 50 to 60 μm because this depth would allow carbides to extend slightly beyond the diffusion zone that would be expected to form after typical PtAl bond coat applications (ref. 4). The goal was to form sub-micron tantalum carbides (TaC) in the superalloy matrix just beneath the diffusion zone, since that was the location for SRZ formation. Additionally, it was desired to carburize the samples using the shortest and lowest temperature soak so that the γ' precipitates in the superalloy matrix would not excessively coarsen.

To assess the effectiveness of the carbide depth, numerous samples were sent to Howmet-Thermatech for application of a commercially-available PtAl bondcoat. After PtAl coating, samples were exposed at GRC to a long-term age in argon of 1093 °C for 400 hr to promote the formation of SRZ. Samples were metallographically prepared and examined through the depth. FESEM was utilized to determine if TaC and/or SRZ were present under the diffusion zone after all processing steps were completed.

Results and Discussion

Surface Finish Study

Table I and figure 6 summarize the surface finishes produced and examined, the corresponding average roughnesses measured, the carbide depths, and the normalized weight gain observed in these slabs after subsequent carburization. Metallographic polishing from 1 to 250 μm produced samples with low surface roughnesses (≤50 nm Ra). Cutting with a fast wafering saw also produced a surface with low roughness (~162 nm Ra). However, grit blasting with different media roughened the surfaces significantly (346 to 1826 nm Ra), and also cleaned the surfaces by removing any oxide scale present. Figure 7 shows views of the deformed surface after grit blasting with the 200 μm Al_2O_3 media. The darker speckles (fig. 7(b)) correspond to Al_2O_3 particles embedded in the alloy. Electron dispersive spectroscopy (EDS) analysis confirmed the presence of Al_2O_3 particles trapped in the deformed surface. The as-received cast slab surface also displayed a high degree of roughness (~1660 nm Ra), since the slabs also received a coarse grit blasting during processing at an outside vendor.

The prepared slab sections were subsequently carburized with a standard cycle containing a 2 hr soak, and the samples were then examined metallographically using FESEM. The microstructures of the samples with low surface roughnesses are displayed in figure 8; these samples exhibited no or minimal carburization near the superalloy surface. The normalized weight gain, reported in table I, was also minimal. The microstructures in figure 8 clearly show the primary phases, namely the γ' precipitate, which is the dark phase that is cuboidal, rounded, or coalesced within the lighter gray matrix of γ.

TABLE I.—SLABS WITH VARIOUS SURFACE TREATMENTS

Surface condition prior to carburization[a]	Average roughness ±95% confidence intervals, nm	Carbide depth ±95% confidence intervals, μm	Normalized wt. gain, mg/cm^2
Polish to 1 μm	5±1.6	0	0.075
Polish to 15 μm (600 grit)	14±0.6	0	0.12
Polish to 250 μm (60 grit)	50±3.3	11±3	0.13
As-cut (SiC-blade)	162±27	0	0.06
Cut + fine blasted	346±22	33±4	0.25
Cut or cast + coarse blasted	1826±95	79±2	0.65
Cut + coarse blasted + fine blasted	1200±48	75±2	0.6
As-received	1660±104	83±7	0.49

[a]Standard carburization condition: 2 hr at 1093 °C

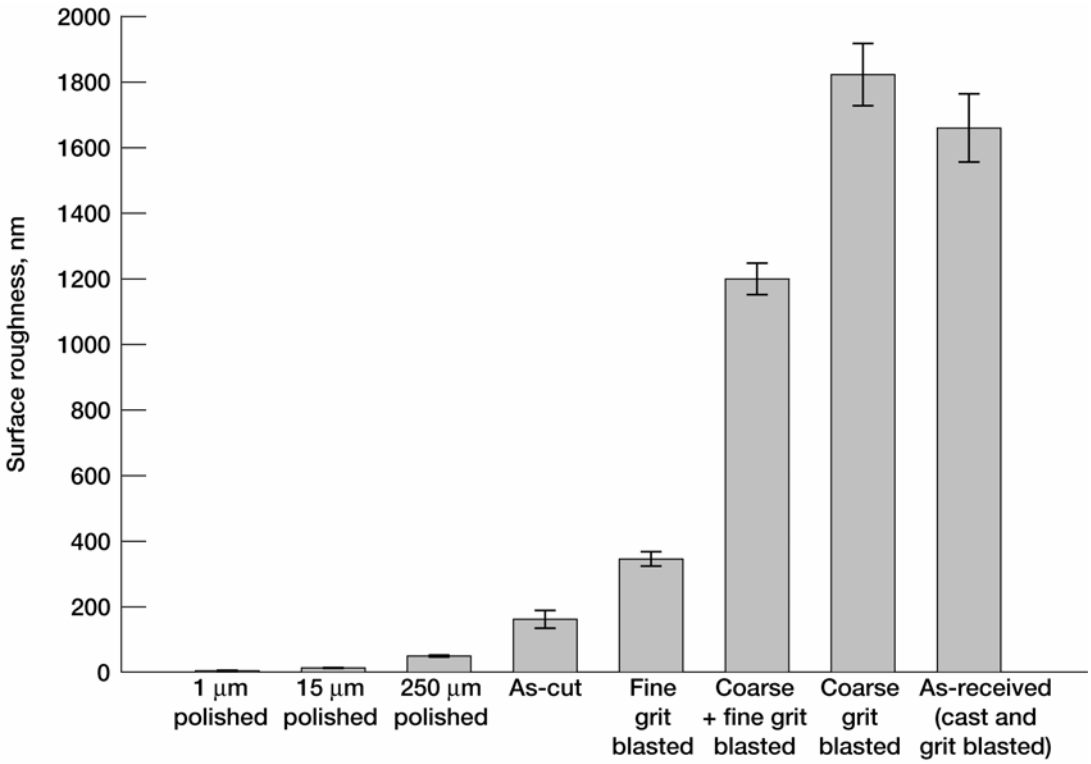

Figure 6.—Surface roughness measurements as a function of surface finish in slab samples.

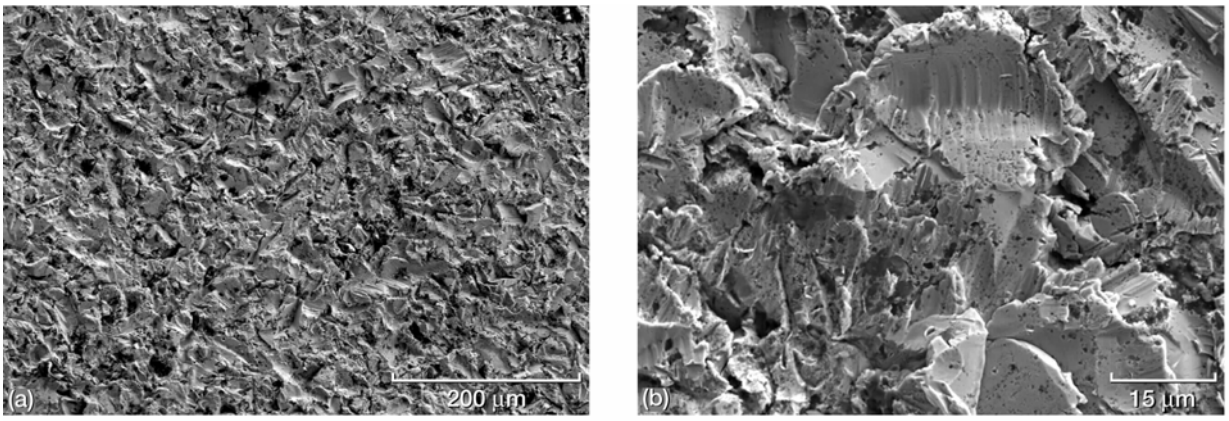

Figure 7.—FESEM images showing superalloy surface after grit blasting using a coarse Al_2O_3 media. (a) Low magnification. (b) High magnification. Darker speckles are mostly Al_2O_3 particles embedded in the deformed surface.

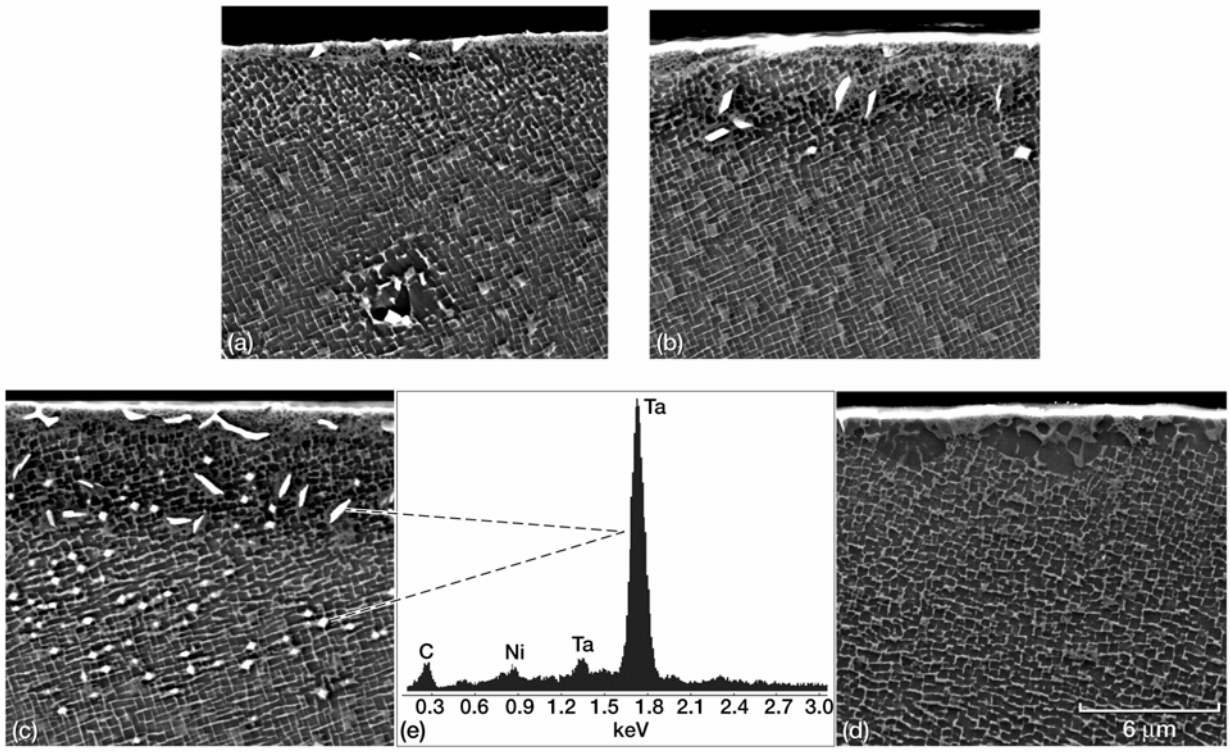

Figure 8.—Typical depths of carbides observed in slabs after carburization at 1093 °C for 2 hr with an initial metallographic polishing. (a) 1 μm. (b) 15 μm. (c) 250 μm. (d) As-cut surface. (e) Typical EDS spectrum of TaC particles.

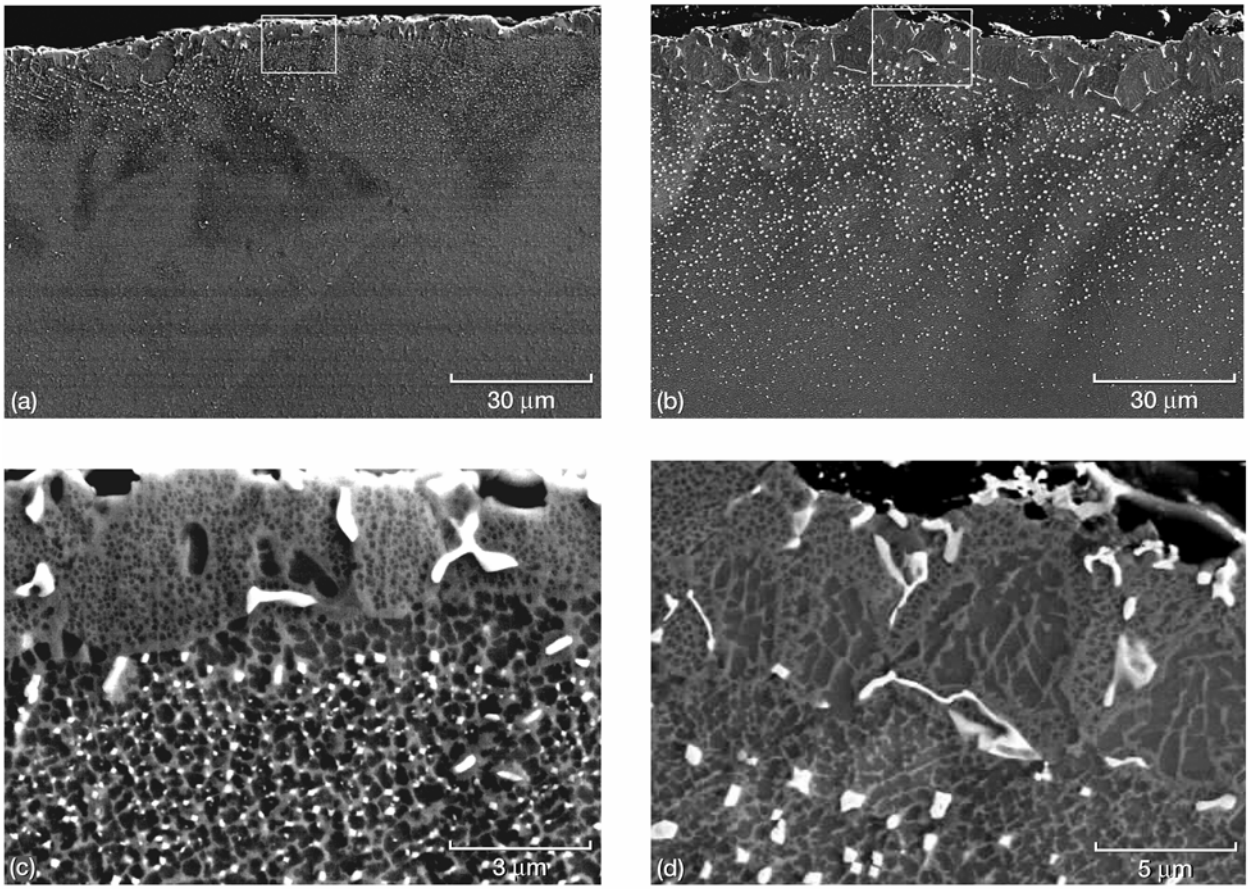

Figure 9.—Typical depths of carbides observed in carburized slab samples at 1093 °C for 2 hr with higher initial surface roughnesses. (a) After fine grit blasting. (b) After coarse grit blasting. (c) Higher magnification near the surface of (a). (d) Higher magnification near the surface of (b).

Recrystallization is evident in figure 8(d) at the surface, and different γ' morphologies are present up to about 6 μm from the surface as compared to those in the internal regions of the same sample. This change in γ' morphology at the surface is evidence that stresses varied along the surface as a result of the preparation technique.

Of greater interest in this study are the few, bright white particles present in some of the microstructures of figure 8. Most of the samples with low roughness values had no carbides or a limited depth of carbides. These bright particles have been analyzed by energy dispersive spectroscopy (EDS) to be rich in tantalum (Ta) and carbon (C) (fig. 8(e)), and are expected to be tantalum carbides (TaC). Figure 8(a) shows a few white TaC particles at the surface, and figures 8(b) and (c) show more diamond-shaped or needle-like white TaC particles beneath the surface. The diamond and plate shapes are believed to be different variants of the carbide. The deepest carbide penetration observed in these samples is only about 10 μm from the surface (fig. 8(c)). The microstructure with the as-cut surface in figure 8(d), with no polishing or blasting, shows no carbide particles at or under the surface.

In contrast, figure 9 depicts typical microstructures in the samples having higher surface roughness prior to carburization. These samples were produced by grit blasting with fine or coarse media. As seen in figures 9(a) to (b), the TaC in these samples is predominantly fine-scale. It is also quite evident that the TaC in these higher surface roughness samples are at a higher overall volume fraction and are present at a greater depth (up to 80 μm), in comparison to the low surface roughness samples in figure 8. The normalized weight gain was consistently higher for the samples with a rougher surface. In addition, the samples in figure 9 exhibited a surface layer of recrystallization or cellular γ', similar to that observed in

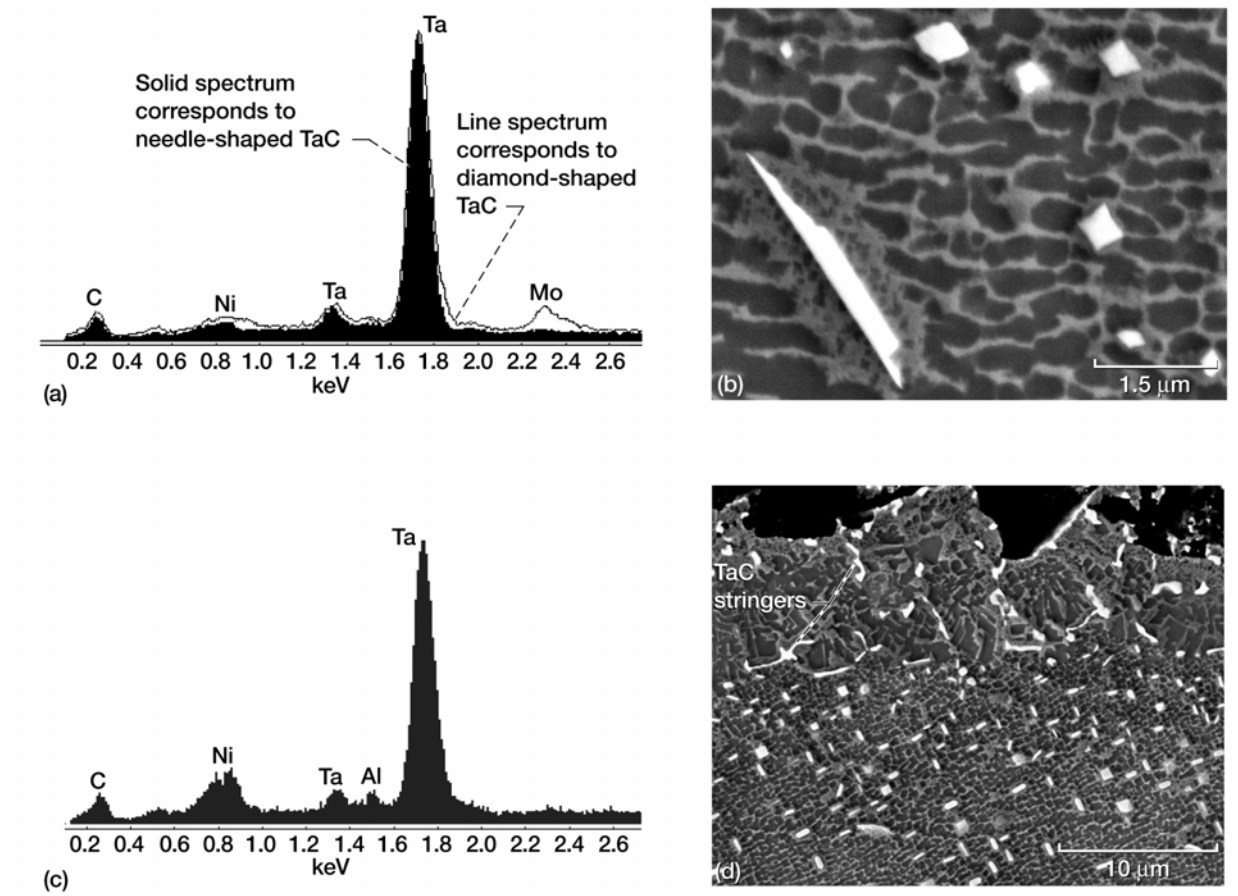

Figure 10.—EDS spectra and images of superalloy surface after coarse grit blasting and carburization. (a) EDS spectrum of needle- and diamond-like TaC shown in (b). (c) EDS spectrum of large stringer-like TaC near surface as shown in (d).

single crystals of similar compositions (refs. 3, 7, and 8). The coarse grit blasting produced a thicker recrystallized layer than the fine grit blasting from the additional cold working of the surface. The interfaces of the individual cells at the surface are partially decorated in the carburized samples in figure 9 with coarse, stringer-like carbides.

EDS spectra shown in figure 10(a) confirm that the diamond and needle-shaped white particles in the superalloy matrix (fig. 10(b)) are mostly rich in Ta and C, and thus are TaC; some contribution from the surrounding matrix is present based on the peaks for nickel (Ni) and molybdenum (Mo). None of the morphologies showed enrichment of Re or tungsten (W), which suggests that TCP was not forming under these conditions. Figure 10(c) is an EDS spectrum of the large stringer-like phase near the superalloy surface (fig. 10(d)). This latter spectrum is also rich in Ta and C, and is very similar to that in figure 10(a). Therefore, it is clear that the white particles present are TaC, which precipitated after the C diffused in from the surface during carburization.

The carbide depths were subsequently measured in the low and high surface roughness specimens using several FESEM micrographs for each surface roughness condition. Magnifications were selected to reveal broad areas with clearly visible carbides. Figure 11(a) displays the measured carbide depths for each surface finish produced. It may be seen in the figure and in table I that the coarse grit blasting, the coarse plus fine grit blasting, and the as-received cast surface were all sufficient to produce the desired carbide depth of about 50 μm or more. Figure 11(b) shows the carbide depth as a function of the average surface roughness and suggests that effective carburization (carbide depths ~50 μm) can be achieved with a surface condition that produces an average roughness of about 1000 nm.

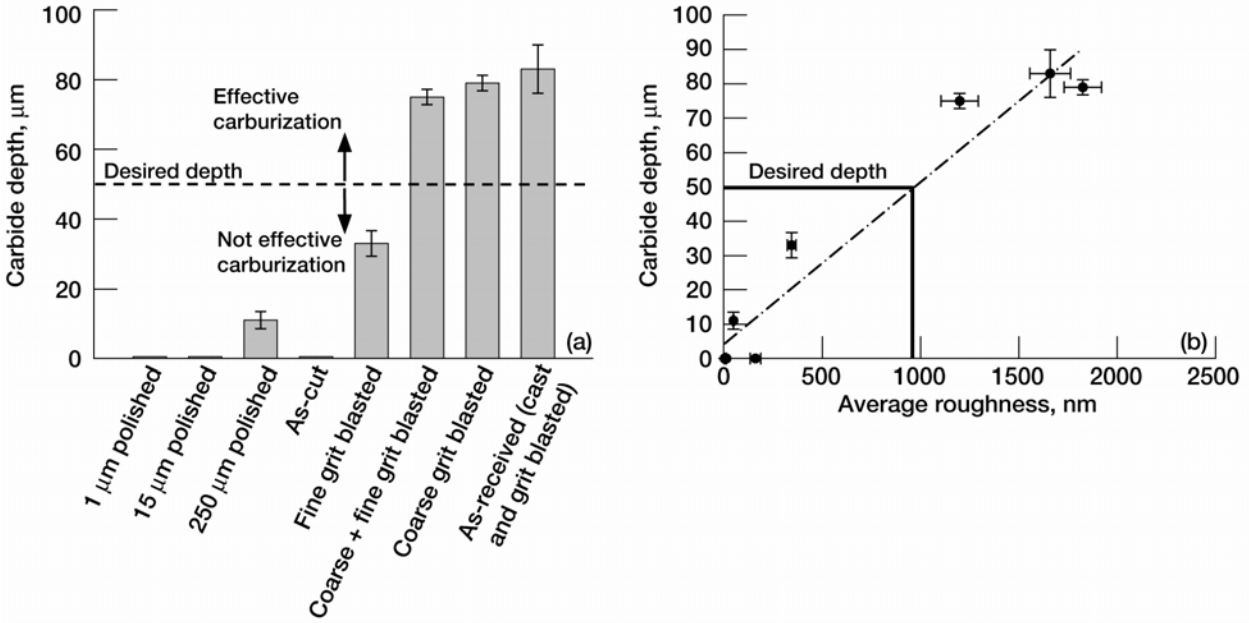

Figure 11.—Carbide depth observed in slab samples of the superalloy. (a) As a function of surface finish. (b) As a function of average surface roughness. The straight line corresponds to a regression analysis with a 95 percent confidence interval.

Alternative Carburization Cycles

Alternative soak times and temperatures for carburization were examined briefly on coarse grit-blasted slab material. Carburization was performed at a lower temperature, in order to reduce the likelihood of γ' coarsening. Minimal or no carburization occurred at 982 °C after a 2 hr soak. Carburization at 1066 °C for 2 hr resulted in carbide depths between 40 to 60 μm for the coarse grit blasted condition and 30 μm for fine blasted surfaces. Longer times of up to 4 hr were also explored at 1093 °C, but this resulted in significantly coarser carbides at depths comparable to the 2 hr soak. Thus, it was determined that the carburization cycle of 2 hr at 1093 °C produced homogeneous and optimal fine-scale carbides with adequate depths.

Carburization of Machined Creep Specimens

It was clear from the surface finish study that the as-machined creep specimens would not carburize without a proper surface treatment. Therefore, a few different surface conditions were produced on machined creep specimens, in order to determine a suitable surface finish for effective carburization. As-machined specimens, machined plus coarse grit blasted, and machined plus stress relief heat treatment (SRHT) plus coarse grit blasted were the surface conditions studied for the machined tensile creep specimens; these surfaces are macroscopically shown in figure 3. The SRHT, which was conducted in argon at 1121 °C for 4 hr, was included in this investigation because it was found (refs. 3 and 4) to be an effective SRZ reduction technique; the SRHT is believed to reduce surface stresses through the recrystallization of the specimen surface. The surface roughness measurements obtained for these various surface finishes are displayed graphically in figure 12. It may be seen that there was a significant difference in the roughness of the as-machined specimen compared to that after coarse grit blasting or after SRHT plus grit blasting.

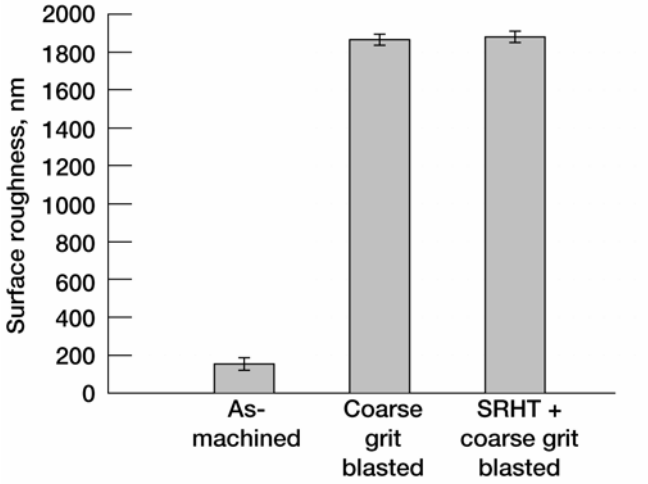

Figure 12.—Surface roughness measurements as a function of surface finish in machined test specimens.

After subsequent carburization with the standard cycle containing a 2 hr soak, the machined samples were examined metallographically using FESEM. The microstructures of these samples near the specimen surfaces are displayed in figure 13. It is clearly evident that the as-machined specimen shows no carburization at or near the superalloy surface; figure 13(a) shows the γ-γ' microstructure with no third phases present. Significant carburization was exhibited by the machined and coarse grit-blasted specimen, as well as by the SRHT plus grit-blasted machined specimen seen in figures 13(b) and (c). Again, a layer of recrystallization was present at the surface with some coarsened, stringer-like carbides at the cellular interfaces, but high volume fractions of fine-scale carbides dominated the microstructure (fig. 13(c)).

Several FESEM micrographs were used to determine the average carbide depth in the machined test specimens. The SRHT plus coarse grit-blasted specimen had an average depth of fine carbides of 62 μm, whereas coarse grit-blasting (no SRHT) resulted in a carbide depth of only 48 μm. The carbide depths as a function of surface finish are presented in table II and figure 14(a). Figure 14(b) shows the carbide depth as a function of the average surface roughness; these data are scanty and somewhat scatter-prone. The machined specimen data in figure 14 suggest that effective carburization (carbide depths ~50 μm) can be achieved with a surface treatment that produces a surface roughness of about or greater than 1600 nm. Numerous, repeat machined specimens were carburized with a combination of a prior SRHT and coarse grit-blasting; this condition reproducibly yielded fine-scale carbide depths of at least 60 μm, and thus became the standard preparation procedure for machined tensile specimens.

Carburization of Blades

Turbine airfoil sections and whole turbine blades were carburized after different surface preparations in order to determine which preparation technique imparted the most effective carburization in these critical components. As-received blades were carburized in addition to those that were either coarse grit blasted or stress relief heat treated and coarse grit blasted. These surface conditions, along with their respective measured roughness values and subsequent carbide depths after carburization, are summarized in table III. The surface roughness measurements obtained for these finishes are displayed graphically in figure 15. The measured surface roughness of the blades in the various conditions ranged from 775 to 1880 nm, with the coarse grit blasting or SRHT plus grit blasting producing the roughest surfaces. The roughness data from all the specimen types suggest that the grit blasting was the major contributor to the

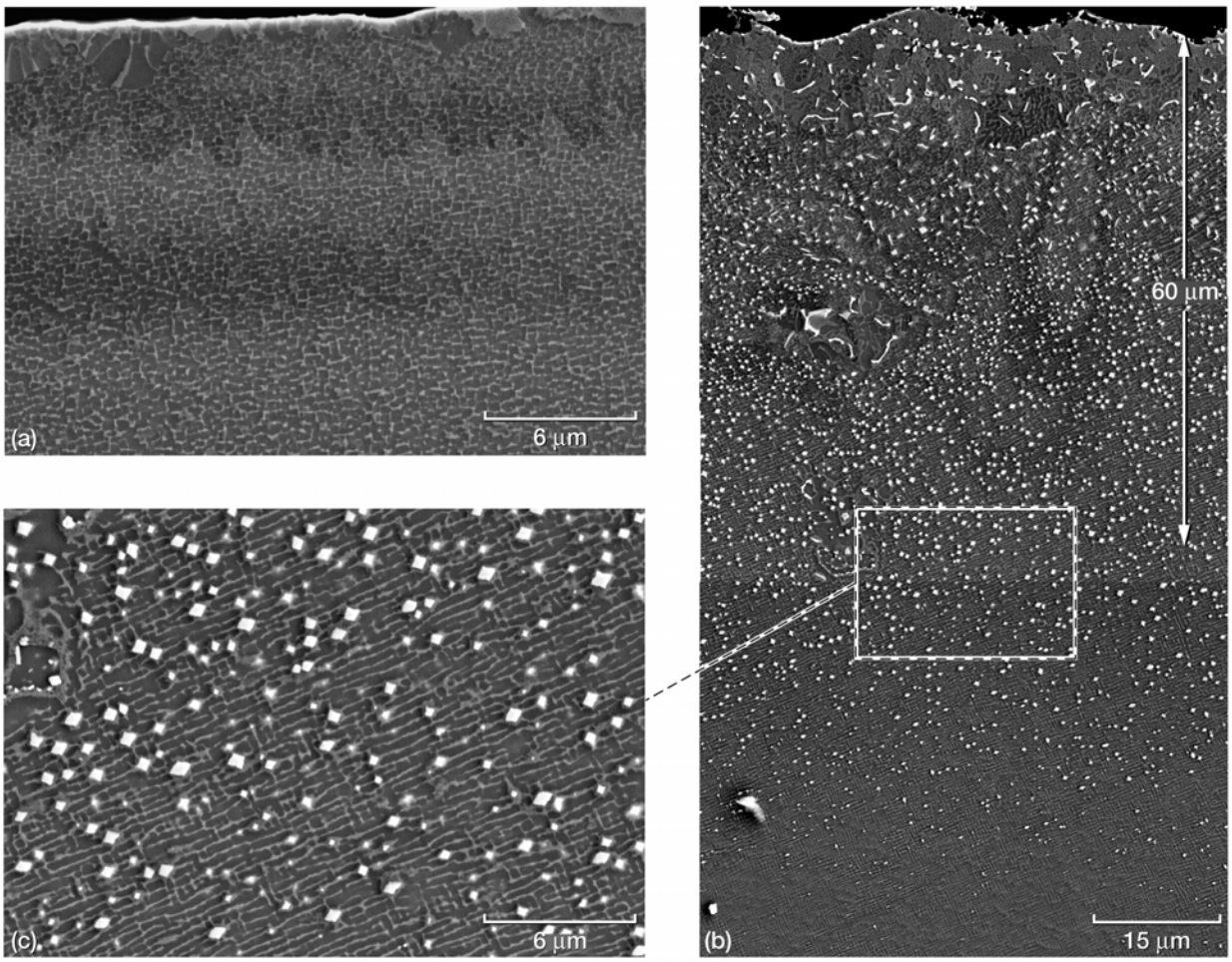

Figure 13.—Cross section views of machined test specimens carburized at 1093 °C for 2 hr. (a) As-machined surface. (b) Stress relief heat treatment and coarse grit blasted condition. (c) Higher magnification of (b) showing a uniform distribution of fine-scale carbides.

TABLE II.—TENSILE CREEP SPECIMENS WITH VARIOUS SURFACE TREATMENTS

Surface condition prior to carburization[a]	Average roughness ±95% confidence intervals, nm	Carbide depth ±95% confidence intervals, μm
As-machined (MA)	154±33	0
MA + coarse blasted	1865±29	48±7
MA + SRHT[b] + coarse blasted	1880±30	62±5

[a]Standard carburization condition: 2 hr at 1093 °C
[b]SRHT = Stress relief heat treatment in argon at 1121 °C for 4 hr

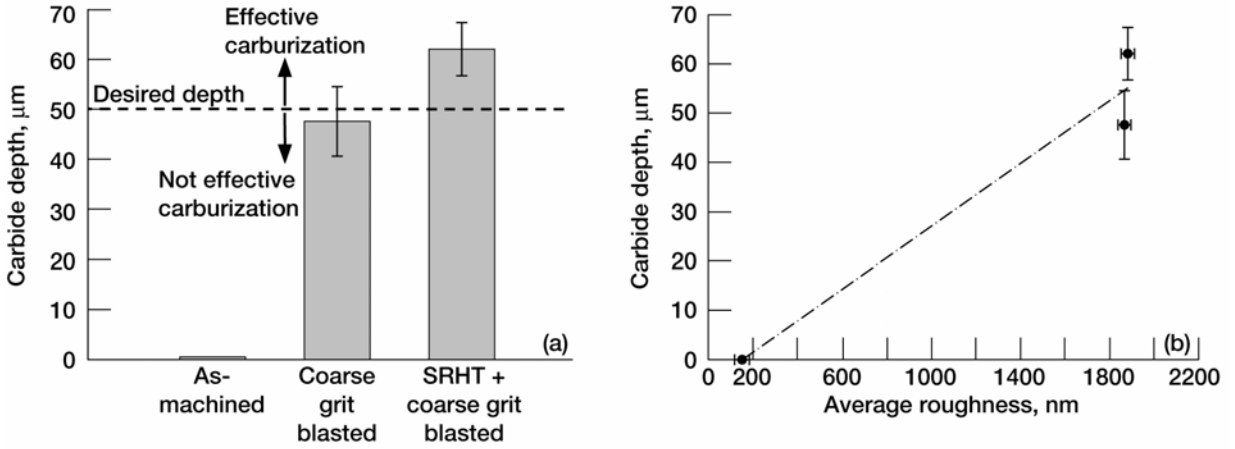

Figure 14.—Carbide depth in machined test specimens of the superalloy. (a) As a function of surface finish. (b) As a function of average surface roughness measured prior to carburization.

TABLE III.—BLADE SECTIONS WITH VARIOUS SURFACE TREATMENTS

Surface condition prior to carburization[a]	Average roughness ±95% confidence intervals, nm	Carbide depth ±95% confidence intervals, µm
As-received blade, pressure side	775±110	87±12
As-received blade, suction side	1242±49	76±9
Any side coarse blasted	1880±58	99±6
Any side SRHT + coarse blasted	1843±64	79±4

[a]Standard carburization condition: 2 hr at 1093 °C
[b]SRHT = Stress relief heat treatment in argon at 1121 °C for 4 hr

final roughness of a specimen prepared for carburization. All specimens, whether slabs, machined tensile specimens, or turbine blades, had a surface roughness between 1826 and 1880 nm after coarse grit blasting. The surface roughness measured on the pressure side of the blades had larger standard deviations than other specimens that were measured. The scatter may be inherent because the measurement itself was more difficult to conduct on this side of the blade due to its concave curvature. The blades underwent many processing steps during manufacturing, including some grit blasting that undoubtedly contributed to the significant roughness values measured in the present study.

After subsequent carburization with the standard cycle containing a 2 hr soak, the airfoil sections were examined metallographically by FESEM. Figure 16 shows the regions near the surface of airfoils that were carburized either in the as-received condition (fig. 16(a)), or after the stress relief heat treatment and coarse grit blasting (fig. 16(b)). In both cases, a layer containing some cellular γ' was present at the surface along with some large, elongated carbides which has been seen previously in grit blasted specimens. However, the carbides that formed beneath the cellular γ'were generally fine scale and were contained in a region up to about 80 µm away from the surface. Closer examination of these carbides revealed that much of their formation was along the thin γ channels between directionally coarsened γ', figure 17(a). The directional coarsening of the γ' indicates that the γ' has lost coherency (refs. 9 to 11) in near surface regions affected by the grit blasting. In regions away from the surface (fig. 17(b)), the γ-γ' microstructure consisted of discrete, sharp, and coherent γ' cuboids separated by very thin channels of γ matrix. No carbides precipitated to these depths.

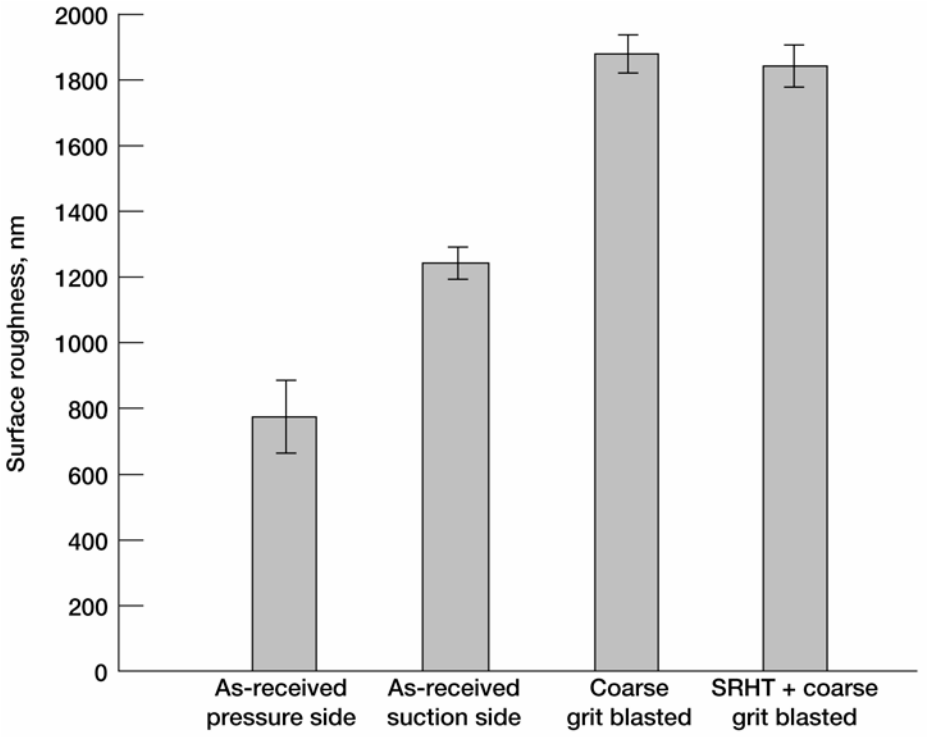

Figure 15.—Surface roughness measurements for turbine airfoils with different surface conditions.

The carbide depths observed in the grit-blasted blades ranged from 79 to 99 μm, whereas the as-received blades had carbide depths up to 87 μm. These data are summarized as a function of surface condition in table III and are plotted graphically in figure 18. Thus, significant carburization occurred in all of these blade surface conditions and all appeared to result in effective carburization. The main difference observed was that the grit blasted blade and the stress relief heat treated and grit blasted blade had carbides that were more coarsened overall, as may be seen in figure 16. In addition, the stress relief and grit blasted blades tended to exhibit more uniform carbide depths along the periphery of the blade section. Thus, it was decided that the most effective carburization in these materials would result from a SRHT at 1121 °C for 4 hr followed by a coarse grit blast prior to carburization.

Effectiveness of Carburization for SRZ Reduction

To test the true effectiveness of these steps for reducing the SRZ instability, full-size blades were processed as described above and then a diffusion aluminide bondcoat was applied on the superalloy. Bondcoats are part of the turbine airfoil system and are added to improve the oxidation resistance of the superalloy and to improve the spallation resistance of the thermal barrier coating. Full-size CF6-80E blades were processed in the following sequence:

(1) SRHT in argon at 1121 °C for 4 hr
(2) Coarse grit blast
(3) Carburization with a 2 hr soak at 1093 °C
(4) Application of a commercially available PtAl bondcoat
(5) Long-term age in argon for 400 hr at 1093 °C
(6) Sectioned along the airfoil span for subsequent metallography

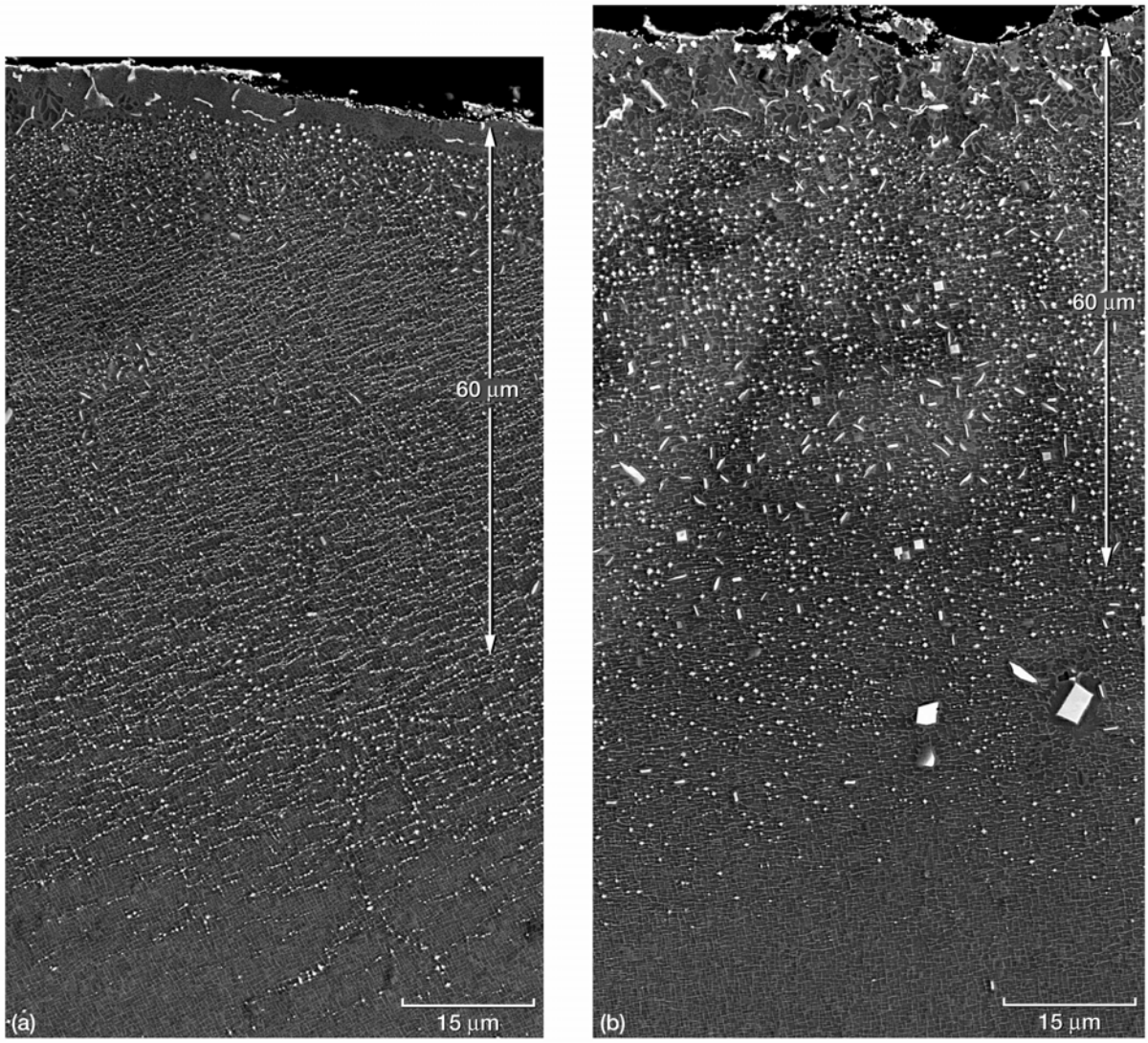

Figure 16.—Montage of FESEM images showing cross sections near the surface of the airfoils that were carburized. (a) As-received condition. (b) After stress relief heat treatment and coarse grit blasting.

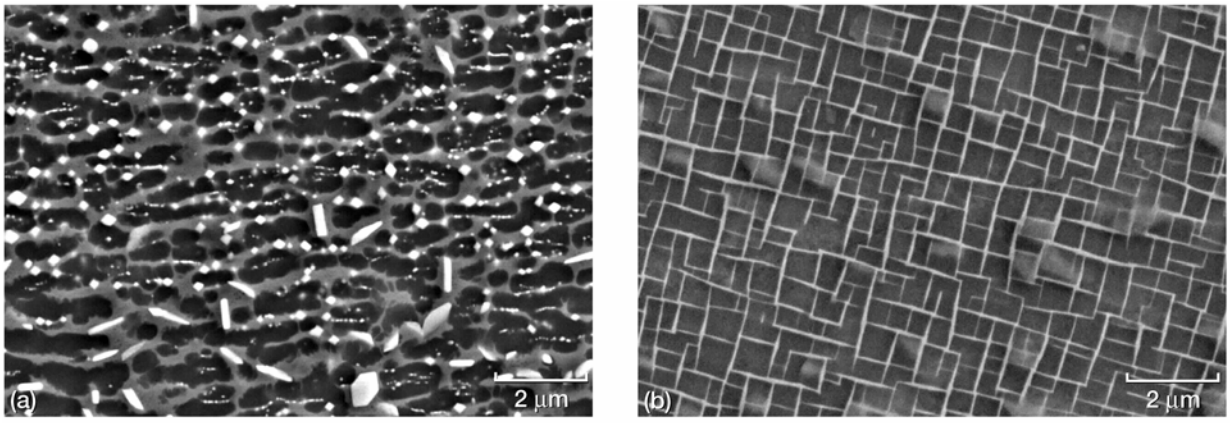

Figure 17.—(a) Typical carbide morphologies observed near the surface of an airfoil after a stress relief heat treatment, coarse grit blasting and carburization at 1093 °C for 2 hr. (b) γ/γ' phase morphology observed in regions away from the surface.

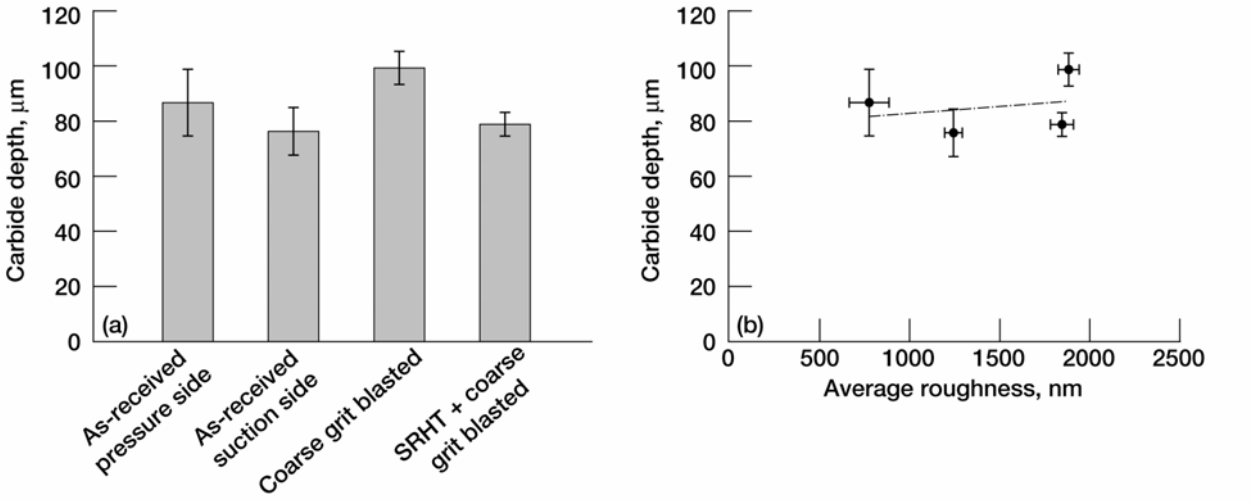

Figure 18.—Carbide depth observed in turbine airfoil sections of the superalloy. (a) As a function of surface finish. (b) As a function of average surface roughness prior to carburization.

The long-term age was applied to further promote the formation of SRZ. These blades will be referred to in the remainder of the paper as the blades with "all fixes." For comparison, full-size CF6-80E blades were also processed with no steps designed to reduce SRZ. These latter blades were processed with only the commercially available PtAl bondcoat and the long-term age for 400 hr at 1093 °C. These blades will be referred to as the "unfixed" blades.

Figure 19 shows a view of the CF6-80E blade with no fixes. The corresponding microstructures of various sections (a, b, and c) throughout the airfoil span are shown on the right of the figure after long-term aging at 1093 °C. The bondcoat is present in the outer ~40-µm-thick layer of the microstructure; it is composed primarily of NiAl grains and fewer grains of γ'. The diffusion zone lies beneath the bondcoat and is approximately 35 µm thick. The diffusion zone develops from interdiffusion between the bondcoat and the superalloy, and consists of blocky TCP and occasional TaC in primarily a matrix of γ' grains. The superalloy lies directly beneath the diffusion zone, and it is in the superalloy regions adjacent to the diffusion zone that the SRZ can be readily observed if no fixes are employed (fig. 19). TCP laths are also present beyond and in between the pools of SRZ. Thus, it is apparent that blades of this advanced superalloy readily develop the potentially deleterious SRZ after bondcoat application and a high temperature exposure if no fixes are applied.

Figure 20 shows a view of the CF6-80E blade with all the fixes. The corresponding microstructures of the sections throughout the airfoil span are shown after long-term aging on the right of the figure. The bondcoat is present in the outer ~50-µm-thick layer of the microstructure and forms martensitic platelets within the NiAl grains. The diffusion zone beneath the bondcoat is well defined and very uniform in thickness (50 µm thick) in this fixed condition. The diffusion zone consists of aligned TCP and fine TaC in primarily a matrix of γ' (figs. 20 and 21(a)). It is clear in figure 20 that no SRZ formed in the superalloy beneath the diffusion zone in any of the sections examined along the blade span. Fine-scale TaC is present in the superalloy regions beneath the diffusion zone (fig. 21(b)) so the desired depth of carbide penetration was achieved. Re-rich TCP is also present beneath the diffusion zone in the form of laths, which may also have contributed to the lack of SRZ by reducing the amount of Re in the matrix. TCP is frequently observed under diffusion zones after coatings are applied, but the presence of TCP is considered to be acceptable (ref. 12) when confined to this location. Thus, it is evident that in the presence of fine-scale TaC and TCP beneath the diffusion zone, SRZ does not form.

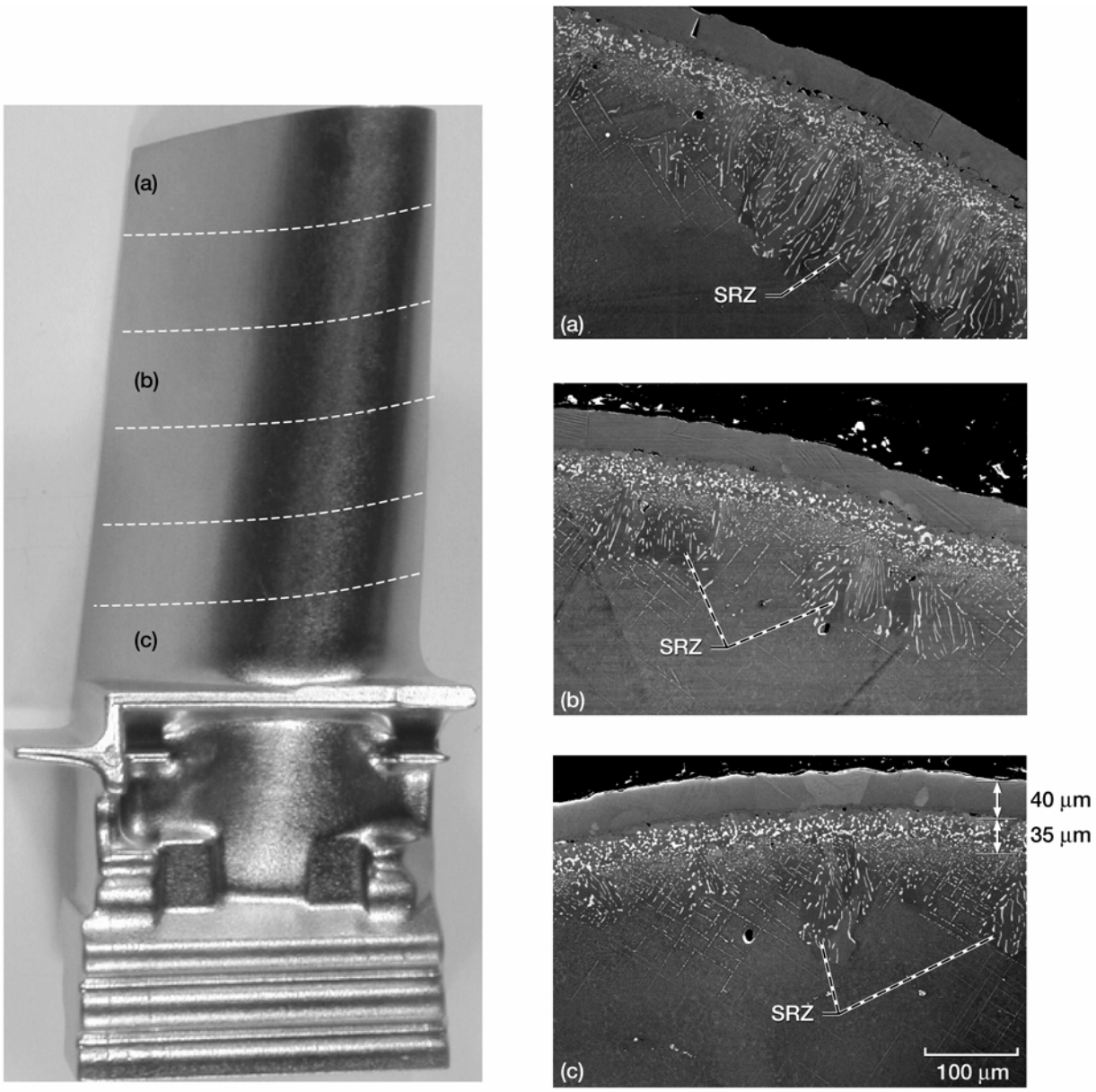

Figure 19.—Full-size blade after application of commercial PtAl bondcoat and aging at 1093 °C for 400 hr. No fixes (SRHT or carburization) were employed prior to bond coat application. Secondary reaction zone (SRZ) is observed in all cross sections (a, b, and c).

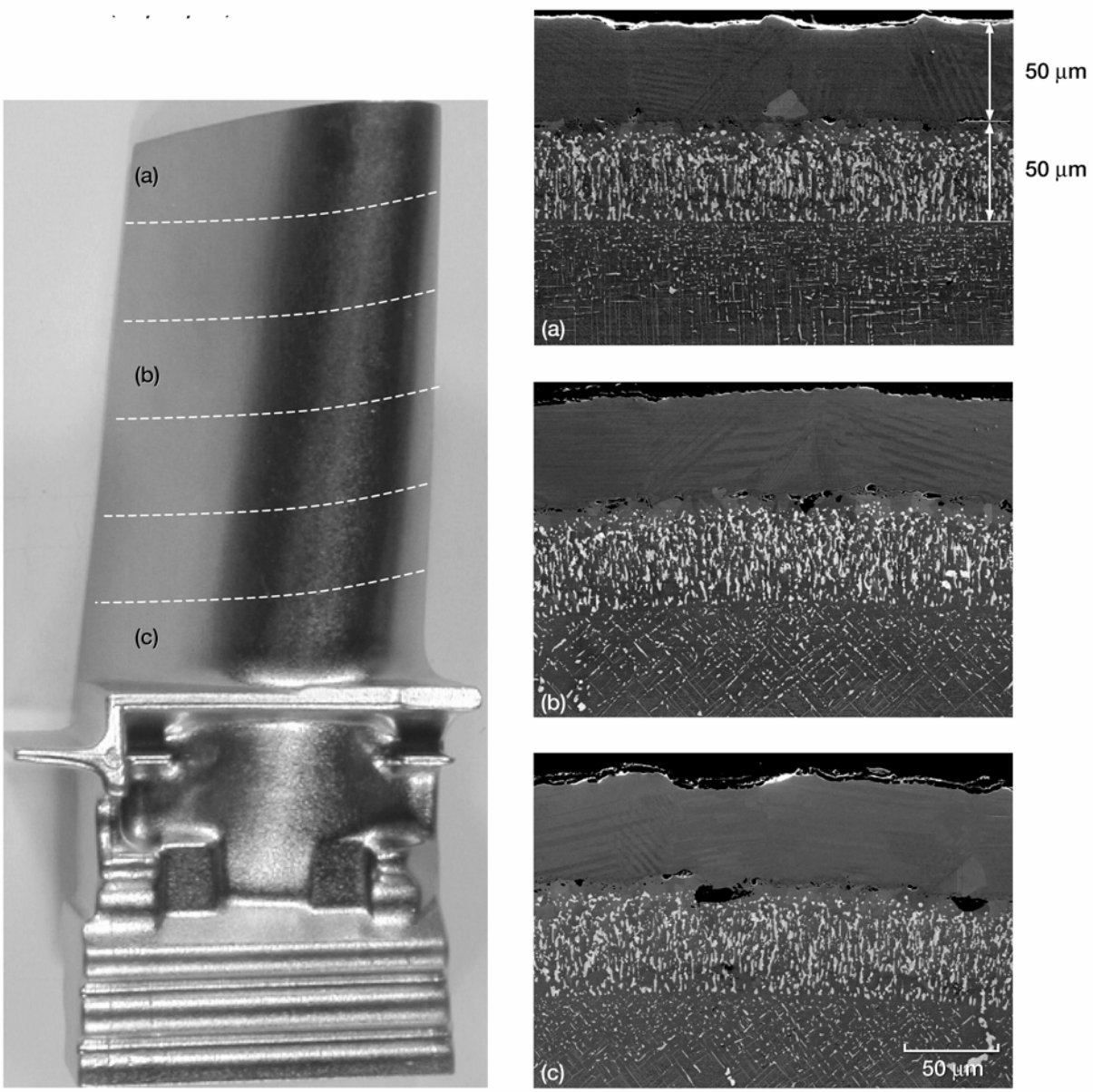

Figure 20.—Full-size blade after stress relief heat treatment, coarse grit blast, carburization, application of PtAl bondcoat, and aging at 1093 °C for 400 hr. No SRZ was observed throughout all the cross sections (a, b, and c) examined.

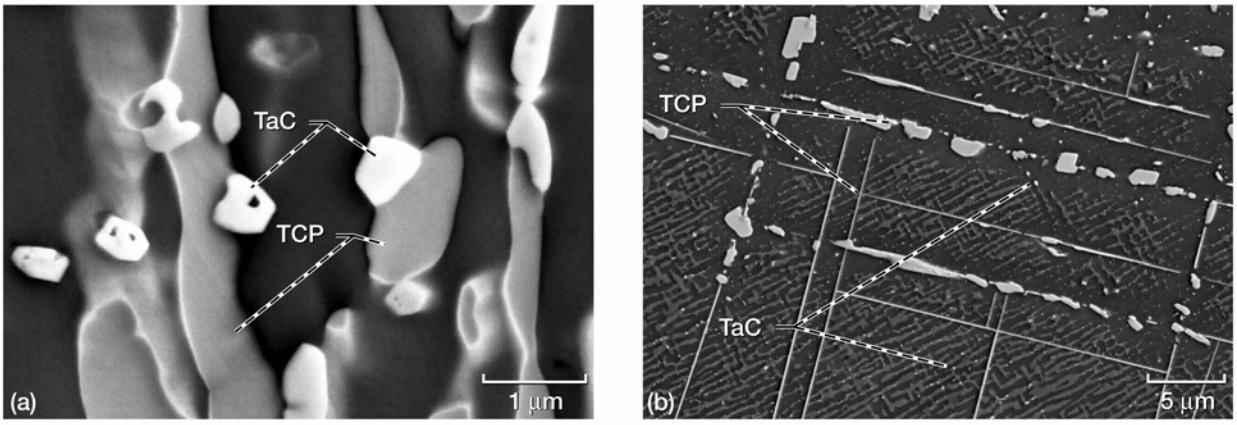

Figure 21.—Images of superalloy blade after stress relief heat treatment and carburization followed by Pt-aluminizing (PtAl) and long-term aging. (a) Diffusion zone. (b) Regions under diffusion zone. Small TaC and TCP platelets are observed in γ/γ' matrix.

The following sequence of steps, performed prior to bondcoat application, was fully successful in eliminating the formation of SRZ in full scale turbine blades of an advanced single crystal superalloy:

(1) SRHT at 1121 °C for 4 hr
(2) Coarse grit blasting
(3) Carburization with a 2 hr soak at 1093 °C

Conclusions

1. Adequate surface preparation is required for effective carburization.

2. Grit blasting with a coarse Al_2O_3 media provided an effective surface condition for subsequent carburization. As-machined test specimens, metallographically polished slabs, and as-cut slab surfaces did not carburize effectively without a prior grit blasting.

3. Stress relief heat treatment of 1121 °C for 4 hr before carburization enhanced the uniformity of subsequent carbide distribution.

4. A carburization cycle consisting of a soak at 1093 °C for 2 hr in a continuously flowing mixture of 3.5% H_2, 0.35% CH_4, and 96.15% Ar provided adequate carbide depths in full size-turbine blades, machined test specimens, and slab material.

5. Fine-scale carbides precipitated at depths that exceeded the thickness of the diffusion zone that later developed after bondcoat application and were found to be effective in eliminating SRZ.

6. Re-rich TCP laths were present in the superalloy beneath the diffusion zone in the blade material. The formation of TCP may have also contributed to the elimination of SRZ by removing Re from the matrix.

Appendix

A.—Commercial procedure for the carburization of advanced superalloys

In order to transfer the carburization technology to commercial vendors, the use of pure hydrogen during the initial steps of the carburization process had to be eliminated. Experiments were designed to eliminate the use of pure hydrogen during the heat-up step, by replacing it with the gas mixture used for carburization (3.5% H_2, 0.35% CH_4, 96.15% Ar). During the early laboratory carburization trials, hydrogen was used to eliminate any possible surface contamination prior to the introduction of the carburization gas mixture. The earlier introduction of the carburization gas mixture, which contains a safe level of hydrogen, has resulted in equally effective results. The system was purged and evacuated prior to heating and leak checked to remove any oxygen that could oxidize the surfaces to be carburized. This process, without the use of hydrogen, is more amenable to many commercial production environments. Sample surface preparation and controlled furnace environment are critical to get consistent carburization results.

B.—Effect of Pre-Aging in H_2 Prior to Carburization

An anneal heat treatment in an inert environment (such as in H_2 or Ar), prior to introducing the carburizing gases, can reduce or prevent the carbide formation. Figure 22 shows a typical microstructure in a sample initially annealed at 1093 °C for 2 hr in a H_2 environment prior to the introduction of the carburizing gas mixture. No TaC was observed after the standard 2 hr carburization cycle, which demonstrates that conditions that enhanced the carburization process have been eliminated. The corresponding EDS spectrum in figure 22 indicates that the white phase is Re-rich and can be clearly differentiated from the Ta peak of an internal TaC formed during the casting process, which has been superimposed in the figure. A γ' cellular microstructure formed near the surface, but no fine carbides were detected beyond the cellular microstructure as compared to samples that were introduced to the carburization environment at an earlier time.

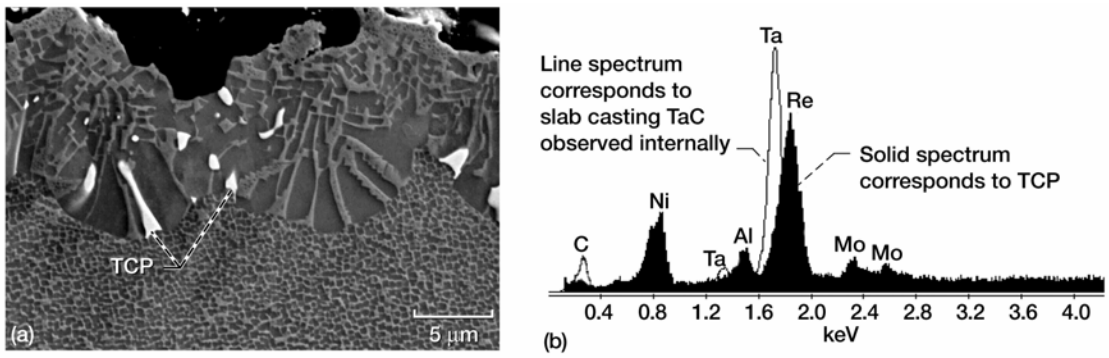

Figure 22.—Image and spectrum of slab sample coarse grit blasted after anneal treatment in H_2 at 1093 °C for 2 hr and then exposed to carburizing environment for another 2 hr. (a) Cross section. (b) EDS spectrum of TCP contained in γ' cellular structure shown in (a).

References

1. W.S. Walston, J.C. Schaeffer, and W.H. Murphy, "A New Type of Microstructural Instability in Superalloys—SRZ," in Superalloys 1996, R.D. Kissinger et al., eds., The Minerals, Metals & Materials Society, 1996, pp. 9–18.

2. W.S. Walston, K.S. O'Hara, E.W Ross, T.M. Pollock, and W.H. Murphy, "René N6: Third Generation Single Crystal Superalloys," in Superalloys 1996, R.D. Kissinger et al., eds., Minerals, Metals & Materials Society, 1996, pp. 27–34.

3. Enabling Propulsion Materials Program: Final Technical Report, Volume 4, Task J-long-Life Turbine Airfoil Materials System, 01 October 1998 to 31 October 1999, NASA Contract NAS 3–26385, May 2000.

4. R.A MacKay, A. Garg, F.J. Ritzert, and I.E. Locci, "Assessment of Creep Capability of HSR–EPM Turbine Airfoil Alloys, NASA Technical Memorandum UEET001," February 2001.

5. J.C. Schaeffer, U.S. Patent 5,334,263, "Substrate Stabilization of Diffusion Aluminide Coated Nickel-Base Superalloys," 1994.

6. American National Standard, "Surface Texture, Surface Roughness, Waviness and Lay," published by The American Society of Mechanical Engineers, ANSI B46.1–1978, New York, NY, pp. 1–35.

7. R.A. MacKay and F.J. Ritzert, "Characterization of GE Blades and Creep Specimens," Presentation at HSR-EPM Team Meeting, NASA Glenn Research Center, Cleveland, OH, November 17, 1998.

8. R.A. MacKay, A. Garg, and F.J. Ritzert, "Microstructural Observations for SRZ Designed Experiments," Presentation at HSR–EPM Team Meeting, NASA Glenn Research Center, Cleveland, OH, July 19, 1999.

9. R.A. MacKay and M.V. Nathal, "γ' Coarsening in High Volume Fraction Nickel-Base Alloys," Acta Metal. Mater., vol. 38, no. 6, 1990, pp. 993–1005.

10. T.P. Gabb, S.L. Draper, D.R. Hull, R.A. MacKay, and M.V. Nathal, "The role of Interfacial Dislocation Networks in High Temperature Creep of Superalloys," Mater. Sci. Eng., vol. A118, 1989, pp. 59–69.

11. M.V. Nathal, R.A. Mackay, and R.G. Garlick, "Lattice Parameter Variations during Aging in Nickel-Base Superalloys," Scripta metall., vol. 22, 1988, pp. 1421–1424.

12. K. O'Hara, personal communication with R.A. MacKay, January 1999.

REPORT DOCUMENTATION PAGE

Form Approved
OMB No. 0704-0188

1. AGENCY USE ONLY (*Leave blank*)	2. REPORT DATE	3. REPORT TYPE AND DATES COVERED
	March 2004	Technical Memorandum

4. TITLE AND SUBTITLE

Successful Surface Treatments for Reducing Instabilities in Advanced Nickel-Base Superalloys for Turbine Blades

5. FUNDING NUMBERS

WBS–22–714–30–09

6. AUTHOR(S)

Ivan E. Locci, Rebecca A. MacKay, Anita Garg, and Frank Ritzert

7. PERFORMING ORGANIZATION NAME(S) AND ADDRESS(ES)

National Aeronautics and Space Administration
John H. Glenn Research Center at Lewis Field
Cleveland, Ohio 44135–3191

8. PERFORMING ORGANIZATION REPORT NUMBER

E–14360

9. SPONSORING/MONITORING AGENCY NAME(S) AND ADDRESS(ES)

National Aeronautics and Space Administration
Washington, DC 20546–0001

10. SPONSORING/MONITORING AGENCY REPORT NUMBER

NASA TM—2004-212920

11. SUPPLEMENTARY NOTES

Ivan E. Locci, Case Western Reserve University, Cleveland, Ohio 44106; Rebecca A. MacKay and Frank J. Ritzert, NASA Glenn Research Center; and Anita Garg, University of Toledo, Toledo, Ohio 43606. Responsible person, Ivan E. Locci, organization code 5120, 216–433–5009.

12a. DISTRIBUTION/AVAILABILITY STATEMENT

Unclassified - Unlimited
Subject Categories: 01, 07, 23, 26, and 31 Distribution: Nonstandard

Available electronically at http://gltrs.grc.nasa.gov

This publication is available from the NASA Center for AeroSpace Information, 301–621–0390.

12b. DISTRIBUTION CODE

13. ABSTRACT ***(Maximum 200 words)***

An optimized carburization treatment has been developed to mitigate instabilities that form in the microstructures of advanced turbine airfoil materials. Current turbine airfoils consist of a single crystal superalloy base that provides the mechanical performance of the airfoil, a thermal barrier coating (TBC) that reduces the temperature of the base superalloy, and a bondcoat between the superalloy and the TBC, that improves the oxidation and corrosion resistance of the base superalloy and the spallation resistance of the TBC. Advanced nickel-base superalloys containing high levels of refractory metals have been observed to develop an instability called secondary reaction zone (SRZ), which can form beneath diffusion aluminide bondcoats. This instability between the superalloy and the bondcoat has the potential of reducing the mechanical properties of thin-wall turbine airfoils. Controlled gas carburization treatments combined with a prior stress relief heat treatment and adequate surface preparation have been utilized effectively to minimize the formation of SRZ. These additional processing steps are employed before the aluminide bondcoat is deposited and are believed to change the local chemistry and local stresses of the surface of the superalloy. This paper presents the detailed processing steps used to reduce SRZ between platinum aluminide bondcoats and advanced single crystal superalloys.

14. SUBJECT TERMS

Turbine airfoil materials; Thermal barrier coating (TBC); Bondcoat; Secondary reaction zone (SRZ)

15. NUMBER OF PAGES

28

16. PRICE CODE

17. SECURITY CLASSIFICATION OF REPORT	18. SECURITY CLASSIFICATION OF THIS PAGE	19. SECURITY CLASSIFICATION OF ABSTRACT	20. LIMITATION OF ABSTRACT
Unclassified	Unclassified	Unclassified	